

In-field methods for rapid detection of frost damage in Australian dryland wheat during the reproductive and grain-filling phase

Authors: Perry, Eileen M., Nuttall, James G., Wallace, Ashley J., and Fitzgerald, Glenn J.

Source: Crop and Pasture Science, 68(6) : 516-526

Published By: CSIRO Publishing

URL: <https://doi.org/10.1071/CP17135>

In-field methods for rapid detection of frost damage in Australian dryland wheat during the reproductive and grain-filling phase

Eileen M. Perry^{A,C}, James G. Nuttall^B, Ashley J. Wallace^B, and Glenn J. Fitzgerald^B

^ADepartment of Economic Development Jobs, Transport and Resources, Cnr Midland Highway and Taylors Street, Epsom, Vic. 3551, Australia.

^BGrains Innovation Park, Department of Economic Development Jobs, Transport and Resources, 110 Natimuk Road, Horsham, Vic. 3400, Australia.

^CCorresponding author. Email: eileen.perry@ecodev.vic.gov.au

Abstract. Frost damage causes significant production losses and costs to Australian dryland wheat, and frost impacts are not expected to decline in the near future, despite global warming. Rapid estimation of frost damage to crops on a spatial basis would allow for timely management decisions to reduce the economic impact of frost events. In this paper, we take a first step in evaluating the utility of hyperspectral reflectance and active light fluorescence for detecting frost damage to wheat during its reproductive phase. Two experiments were conducted immediately after the first observation of frost damage, (i) in 2006, five plots in an existing trial were opportunistically subdivided to take spectral reflectance measurements on frost damaged plants along with yield measurements, and (ii) in 2015, a transect across 31 rows within a commercial paddock was established to evaluate spectral reflectance, fluorometer measurements, and yield along a gradient from non-frosted to frost damaged plants. The results of the hyperspectral reflectance data appeared variable in response across the two experimental sites where frost was observed in-crop. In 2006, hyperspectral-derived indices showed significant differences ($P < 0.05$) between measurements of frosted and non-frosted canopies, but this was not the case for observations taken in 2015, where the mean response was reversed between experimental sites for several of the indices. In contrast, fluorometer measurements in the 2015 trial resulted in higher correlations with yield and observed frost damage compared with the reflectance measurements. Seven of the nine fluorometer indices evaluated were correlated with yield (used as an indicator of frost damage) at $P < 0.01$. An index of compounds which absorbs at 375 nm, FLAV, had the best correlation coefficients of 0.91 and 0.90 for the two dates in 2015. The fluorescence index FLAV was selected to evaluate whether it could be used to classify the canopy as frost affected or not, using discriminant analysis for the 2015 transect data. The overall classification accuracy, defined as the number of correctly classified measurements (57) divided by the total number (62) was 92%. The present study was not able to provide insight into how rapidly the sensors could detect frost damage before detection with the naked eye, as the survey data constituted a transect based on early visual symptoms, however this study does provide important insight into what sensors and/or indices may be sensitive to 'seeing' early frost damage in-crop. The next steps, which build on this work and need to be resolved are (i) what is the nominal scale of measurements required, and for which portions of the plant canopy? (ii) How robust (over space and time) are any relationships between frost damage and index response? (iii) Can frost damage be detected before the onset of visual damage?

Additional keywords: fluorometer, proximal sensing, spectral reflectance.

Received 1 April 2017, accepted 10 June 2017, published online 11 July 2017

Introduction

Impacts and cost of frost damage to wheat in Australia

Frost damage causes production losses and costs to Australian dryland crops, economic losses due to frost damage to wheat have been estimated up to \$100 million per year (Juttner 2014). Zheng *et al.* (2012) analysed weather data from 1960 to 2009 for 2684 weather stations across Australia, and showed that most of the Australian wheatbelt experienced winter or spring frost events with major portions (Victoria, New South Wales, southern

Queensland, and inland parts of South Australia) having recorded frost temperatures ($< 0^{\circ}\text{C}$) in 80% or more of the years for that period. Zheng *et al.* (2015) analysed gridded weather data across Australia from 1957 to 2013, and found that some frost-prone areas of the Australian wheatbelt were exposed to an increase in the number of frost events, and a delay in the last frost date. Likewise, observational data supports an increase in the number of frost events (Wahlquist 2012). Continued increased warming due to global warming is expected to increase the risk of post-head

emergence damage due to accelerating wheat phenology, leading to heading occurring during frost periods (Wang *et al.* 2015). Thus, the impact and cost due to frost is not expected to decline with increased global warming in the near future. Increased frequency of clear skies and heat loss across many arable cropping regions are likely to dominate over effects of average ambient temperature increases associated with increasing atmospheric CO₂ concentration.

Although frost damage can occur any time following emergence, the frost damage to wheat during ear emergence and early anthesis is considered the most damaging to grain yield (White, GRDC and Agriculture Western Australia 2000). Frost can cause death of anthers and embryos (Cromeley *et al.* 1998), resulting in sterility of florets and whole spikelets (Marcellos and Single 1984; Al-Issawi *et al.* 2013), thereby impacting yield. Visible symptoms may include bleaching of awns and anthers, which become pale yellow or white and shrivelled. Over time, grain will not form in frosted florets, which may appear bleached and shrivelled, and grain in part or whole of heads will not form (White, GRDC and Agriculture Western Australia 2000).

Agronomic management of wheat to reduce frost damage is challenging, as the severity of the impact is influenced by agro-ecological zones and position in the landscape. The major agronomic management tools are planting date and selection of suitable varieties with appropriate phenology to control the flowering window and with an increased tolerance to low temperature. Delayed sowing may reduce the risk of frost damage near anthesis (flowering date), but increase the risk of damage due to heat stress. Thus it is a challenge to growers to navigate extreme temperature effects on production. There is a recognised need to develop new varieties that are less sensitive to frost events (e.g. Zheng *et al.* 2012), but it seems inevitable that frost damage will continue to be a risk factor for wheat. Although not a solution to the problem, post-event frost damage detection and assessment would provide another management option. Rapid estimation of frost damage on a spatial basis could allow for timely management decisions such as salvaging frosted crops for hay, prioritising further crop inputs, altered grain marketing strategies and improved planning of harvest logistics.

Previous research

Remote sensing has demonstrated potential to provide temporal and spatial information on crop damage (e.g. Peters *et al.* 2000; Silleos *et al.* 2002; de Leeuw *et al.* 2014) due to various factors. Data sources include satellite imagery, cameras flown on light aircraft or unmanned aerial vehicles (UAV), and handheld (proximal) sensors. Passive optical sensors such as multispectral or hyperspectral imaging systems that measure light reflected from plant canopies may provide a technology that can detect frost damage in crop before being discernible by the naked eye. Macedo-Cruz *et al.* (2011) classified digital camera images (red, green, blue) taken 15 days after the last frost on an oat crop into classes of healthy, frost damaged (yellow leaves), intermediate damage, and shade. The unsupervised classification techniques were validated against visual inspection of reference plots, and the

technique was found to be robust across illumination conditions (clouds and time of day). However, although this technique provides information on both the location and extent of damage, detection and mapping of the frost damage before visual symptoms are detected would enable more timely action to be undertaken.

The optimal spectral regions for detecting frost damage still need to be defined as little is known about the structural or biochemical changes induced by frost that may be detected as changes in reflectance signatures. Flower *et al.* (2014) found that when compared with the leaves of non-frosted wheat plants, leaves of those that had been subjected to a frost treatment exhibited changes in reflectance between 500–680 nm and 730–740 nm. Wu *et al.* (2012) acquired spectral imagery (400–1000 nm) for potted wheat seedlings on 1–2-week intervals from seedling emergence to the occurrence of freezing injury. Note that in this study they did not report canopy or air temperatures, but acquired measurements over a range of visible damage until all seedlings had died. Overall, the total reflectance (from 400 to 1000 nm) decreased with increased frost exposure over the period from 8 December 2010–17 January 2011. The changes in the average reflectance values were consistent with stressed vegetation: decreasing reflectance in the green and near-infrared regions, and increased reflectance in the red, with a slight shift in the chlorophyll red-edge towards the longer wavelengths.

One promising technology with potential for early detection of crop disorders is fluorescence spectroscopy. Fluorescence is a process by which pigments in plants re-emit absorbed radiation at longer wavelengths than that absorbed. Changes in fluorescence at different wavelengths can be robust indicators of plant responses to specific abiotic stresses (Jones 2014). Fluorescence measurements have been used for wheat to characterise leaf nitrogen (Bürbling *et al.* 2011; Fernandez-Jaramillo *et al.* 2012), and water stress (Bürbling *et al.* 2013). Chlorophyll fluorescence has been shown to relate to freezing tolerance assessments in leaves from wheat (leaves frozen at -15°C) in Rapacz and Woźniczka (2009), and triticale (leaves frozen at air temperatures from -5°C to -20°C) in Rapacz *et al.* (2011). Rizza *et al.* (2001) measured the ratio of variable over maximum fluorescence (Fv/Fm) in young oat plants across a range of winter and spring varieties, hardening treatments (pre-exposure to cold temperatures), a range of freezing temperatures, and days following the freezing event. A freezing treatment (-10°C) caused a dramatic and non-reversible decrease in the ratio of Fv/Fm in plants that had not been cold hardened. A strong correlation ($r = -0.87$) was found between Fv/Fm measurements made immediately after exposure to -12°C , and visual scoring of frost damage in the field for the corresponding cultivars tested. Wu *et al.* (2012) used a handheld active light fluorometer to measure a nitrogen balance index (NBI_G; Ghazlen *et al.* 2010) for potted wheat seedlings exposed to freezing temperatures, and assessed by visual inspection of apparent damage. With accumulation of freezing events, the NBI_G values actually increased, rather than decreased as would be expected. The authors of that study suggested that the stress in the seedlings caused an increase in polyphenol content. The NBI_G used is determined by fluorescence ratios, which depend both on epidermal phenolic compounds and chlorophyll. These results

suggest that in-field fluorescence measurements could be evaluated for characterisation of frost damage in wheat.

Current research and hypotheses

Literature research reveals a gap in the detection and characterisation of frost damage to wheat using non-destructive tools, particularly near the critical anthesis period. The ideal detection method would be effective before the onset of visual symptoms, be applicable across paddocks, and allow spatial management decisions as close to the frost event as possible. In this paper, we take a first step in evaluating hyperspectral reflectance and active light fluorescence for detecting frost damage to wheat during anthesis, exploiting opportunistic datasets measured immediately after the observation of frost damage in the field.

Material and methods

Experimental sites

Horsham plots 2006

Data were utilised from a field experiment in 2006 located near Horsham, Australia (36°44'S, 142°06'E; elevation 133 m). The climate is classified as a semiarid, cold steppe (Peel *et al.* 2007) with frosts often occurring during the reproductive and grain-filling stages of wheat growth. The soils are characterised as grey clays (Vertosol). The original experiment (Fitzgerald *et al.* 2010) was designed to measure canopy nitrogen (N) and water status using reflectance and thermal infrared canopy temperatures on plots with N and two irrigation treatments applied to wheat (*Triticum aestivum* L., cv. Chara). The two N application rates applied were 0 and 39 kg N ha⁻¹. The irrigation amounts applied for the growing season were 142 mm and 275 mm, representing total annual rainfall of 323 mm (decile 4) and 455 mm (decile 7), respectively. A weather station was situated on site, and recorded average air temperature at 1.2 m at 15-min intervals. During the period just before anthesis (24 October 2006) until harvest, there were three natural frost events. These events occurred 10, 22, and 29 October 2006, with minimum temperatures recorded of -1.7, -1.4, and -1.4°C, and cold sums of 2.6, 1.6, and 1.5°C.h (<0°C), respectively. Although the temperatures were recorded on site, slight variations in micro relief may have produced local differences in chilling severity.

Frost damage was first observed on portions of five of the eight rainfed plots on 24 October, which coincided with wheat at mid-flowering (Z65, Zadoks *et al.* 1974). After frost was observed, the five plots were divided into frosted and non-frosted subplots, and the reflectance measurements were made separately on the frosted and non-frosted subplots. Reflectance measurements for the rain-fed plots were made on 15 September (Z31), 30 September (Z32), 24 October (Z65), and 8 November (Z73). Details of the methods are included in section 2.2. Four of the five frosted subplots were sampled on 8 December (Z92) with biomass cuts taken to determine yield. The subplots were sampled on 8 December (Z92) for grain weight (yield).

Kewell transect 2015

The second dataset was acquired near Kewell, Australia (36°30'S, 142°22'E; elevation 139 m) in 2015 in a commercial field planted to wheat (*Triticum aestivum* L., cv. Wallup). The site

is characterised by grey clays (Vertosol) with a similar climate to Horsham. The annual rainfall was 258 mm. A transect across 31 rows spaced 0.365 m apart was established on 9 October 2015 (Z68), based on an observed gradient of frost from west (healthy plants) to east (visual damage to heads). The transect was marked to allow repetitive measurements. For each of the 31 rows (aligned north-south) across the transect, measurements were made along the row, starting 3 m south of the transect line, and ending at the transect line. Each row was categorised by frost damage: frosted, non-frosted, or transitional. In addition, 11 rows were noted as impacted by wheel tracks, or heavy stubble.

For the Kewell transect, in the period between the commencement of wheat heading to 10 days after anthesis there were two natural frost events, where minimum temperatures were -1.5 and -2.1°C for the 23 and 29 September respectively, measured at 1.2 m at 5-min intervals. Cold sums for these respective events were 4.2 and 5.3°C.h (<0°C). These canopy temperatures were recorded ~15 m from the transect location, where variations in micro relief and the flow of cold air to the lower lying portion of the transect (eastern end), would have produced a local differential in chilling severity.

Both reflectance and fluorescence measurements were made on the transect during October 2015; details of the sensors are included in section 2.2. Fluorescence measurements for the transect were made 9 October (Z68) and 13 October 2015 (Z71-Z75). Reflectance measurements were also made on 13 October. Biomass cuts for each of the 31 rows were collected to determine aboveground biomass and yield components.

Sensors used

Portable spectrometer

Canopy reflectance measurements were made during 2006 and 2015 using a portable spectrometer (Field Spec FR, ASD Inc., Boulder, CO, USA), resulting in libraries of spectra from 350 to 2500 nm, sampled to a 1-nm resolution. The measurements were made using no fore-optic; the fibre optic has a field of view of ~25 degrees. Measurements were made by positioning the fibre optic above the canopy, resulting in a ground sample diameter of ~1 m for each spectrum. The spectra were captured as reflectance values, calibrated against a Spectralon® target representing 100% reflectance across all wavelengths. Following the field measurements, the spectra were processed and spectral indices were generated. The full spectra were subset to facilitate processing without affecting the computation of indices. Each spectrum was resized by removing every other wavelength, which maintained the nominal spectral resolution of the instrument. Spectral regions with relatively low signal to noise, due to a combination of instrument and atmospheric effects, were removed. These regions were 1750–1950 nm, and all values at wavelengths longer than 2300 nm. To further reduce artefacts of illumination, continuum removal was used to normalise spectra across datasets (Kokaly and Clark 1999). A suite of indices were generated from the normalised spectra as shown in Table 1. The indices represent a selection for sensitivity to chlorophyll concentration (CI, MCARI, NDRE, CCCI, RVSI), water stress (WI), canopy cover and canopy structure (NDVI, EVI, SIPI), plant senescence (PSRI), cellulose and leaf moisture (CAI), and photochemical response (PRI).

Table 1. Spectral indices computed from reflectance measurements

Index	Formula	Reference
Canopy Chlorophyll Concentration Index (CCCI)	Based on Normalised Difference Vegetation Index (NDVI) and Normalised Difference Red-Edge (NDRE) Index, below	Fitzgerald <i>et al.</i> (2010)
(Modified) Cellulose Absorption Index, CAI	$0.5(R_{2.0} + R_{2.2}) - R_{2.1}$	Daughtry (2001)
Chlorophyll Index Red-edge, CI	$(RNIR/NRE) - 1$	Gitelson <i>et al.</i> (2006)
Enhanced Vegetation Index, EVI	$G*(NIR - R)/(NIR + 6*R - 7.5*B + 1)$	Huete <i>et al.</i> (2002)
Modified Chlorophyll Absorption Reflectance Index, MCARI	$((R_{700} - R_{670}) - 0.2*(R_{700} - R_{550}))* (R_{700}/R_{670})$	Daughtry <i>et al.</i> (2000)
Normalised Difference Red-Edge Index, NDRE	$(R_{800} - R_{720})/(R_{800} + R_{720})$	Clarke <i>et al.</i> (2001)
Normalised Difference Vegetation Index, NDVI	$(R_{800} - R_{670})/(R_{800} + R_{670})$	Rouse <i>et al.</i> (1974)
Photochemical Response Index, PRI	$(R_{570} - R_{531})/(R_{570} + R_{531})$	Gamon <i>et al.</i> (1992)
Plant Senescence Reflectance Index, PSRI	$(R_{680} - R_{500})/R_{750}$	Merzlyak <i>et al.</i> (1999)
Red-edge Vegetation Stress Index, RVSI	$((R_{712} - R_{752})/2) - R_{732}$	Merton (1998)
Structure Insensitive Pigment Index, SIPI	$(R_{800} - R_{445})/(R_{800} - R_{680})$	Penuelas <i>et al.</i> (1995)
Water Index, WI	R_{900}/R_{970}	Penuelas <i>et al.</i> (1997)

Table 2. Indices determined from fluorometer measurements

Index	Formula	Description
ANTH_RB	Log (InfraRed Fluorescence excited with Red/InfraRed Fluorescence excited with Blue)	Index of anthocyanin. If there is no anthocyanin, index negatively correlated with chlorophyll
ANTH_RG	Log (InfraRed Fluorescence excited with Red/InfraRed Fluorescence excited with Green)	Index of anthocyanin. If there is no anthocyanin, index negatively correlated with chlorophyll
BFRR_uv	Yellow (Blue) Fluorescence excited with UV (375 nm)/InfraRed Fluorescence excited with UV (375 nm)	Demonstrated response to drought stress in wheat (Bürling <i>et al.</i> 2013)
FLAV	Log (InfraRed Fluorescence excited with Red/InfraRed Fluorescence excited with UV (375 nm))	Index of compounds which absorbs at 375 nm
NBL_G	InfraRed Fluorescence excited with UV (375 nm)/Red Fluorescence excited with Green	Nitrogen Balance Index
NBL_R	InfraRed Fluorescence excited with UV (375 nm)/Red Fluorescence excited with Red	Nitrogen Balance Index
NBI1	$(\text{InfraRed Fluorescence excited with UV (375 nm)} * \text{InfraRed Fluorescence excited with Green}) / (\text{Red Fluorescence excited with Red})^2$	Nitrogen Balance Index 1 (Agati <i>et al.</i> 2013)
SFR_G	InfraRed Fluorescence excited with Green/Red Fluorescence excited with Green	Index of chlorophyll
SFR_R	InfraRed Fluorescence excited with Red/ Red Fluorescence excited with Red	Index of chlorophyll

Active light fluorometer

A handheld active light fluorometer (Multiplex 3.6, Force A, Orsay Cedex, France) with four excitation bands (UV, blue, green, and red) and three detection bands (yellow, red and far red) was used in 2015. The fluorometer measurements resulted in a suite of indices from various combinations of the activation and detection wavelengths used (e.g. Ghazlen *et al.* 2010), as shown in Table 2. Measurements were made to target the heads and top of the wheat canopy. As this instrument is a proximal sensor; the sensor was operated so the wheat heads just brushed the face plate (aperture) of the instrument as the operator walked along each of the 31 rows of the transect. The 8-cm aperture plate was used. Following data acquisition, processing was performed to screen measurements with low signal to noise according to the manufacturer guidelines.

Statistical analyses

The GENSTAT statistical analysis software package (VSN International 2011) was used to perform ANOVA and discriminant analysis for the datasets.

Results and discussion

Frost effects on yield

Both the 2006 and 2015 datasets exhibited a decrease in yield following the observed frost damage to the heads. For the Horsham 2006 data, yields for the four plots with observed frost were less than corresponding values for the eight plots without observed frost damage. Likewise, the 2015 transect showed a strong trend from higher yields occurring at the west end, to lower yields at the east end with the greatest visual frost

damage. The 2015 transect was subset for the analysis of means; seven of the rows on the west end were selected to represent non-frosted, and eight rows on the east end were selected to represent frosted samples. The remaining rows out of the 31 were transitional between frosted and non-frosted. The mean yield values and corresponding standard errors, by frost exposure and location, are shown in Fig. 1. The yields were not significantly different for frost effects for 2006 ($P < 0.255$), but were for 2015 ($P < 0.001$) datasets. Nonetheless, the results indicate that the observed frost near anthesis resulted in yield reduction. Although yield reduction was not statistically significant at Horsham, frost

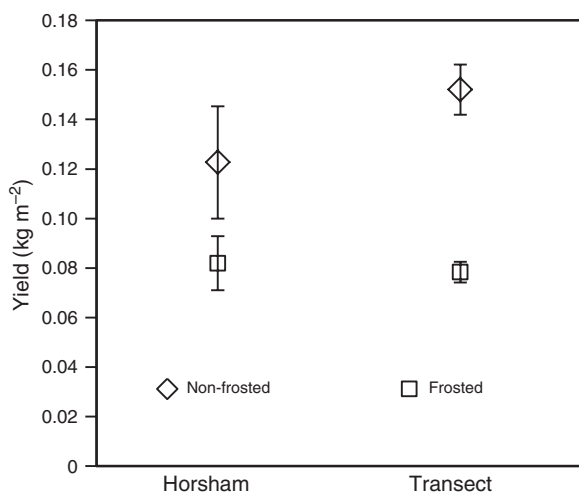


Fig. 1. Wheat grain yields for the 2006 and 2015 datasets indicating the mean and standard error (Horsham $n = 12$, Transect $n = 15$).

damage to heads was readily apparent and useful for establishing spectral signatures.

Canopy reflectance response to frost

Canopy reflectance measurements were made during 2006 and 2015 using a portable spectrometer. Figure 2 shows the reflectance spectra average by site, growth stage, and frost damage (frosted or non-frosted). The spectra acquired in 2006 demonstrated the reflectance changes as the crop matures under drought conditions from Z31 to Z73. Overall, the reflectance in the green and NIR wavelengths decrease, whereas the red reflectance increases. Comparing the spectra for the non-frosted canopies (solid lines) and those measurements on frosted plants (dashed lines) indicate differences for the same crop growth stage. The non-frosted canopy appear to have a deeper absorption feature, that is, lower reflectance values near 680 nm, which is indicative of strong chlorophyll absorption. There are slight differences in the position of the red-edge, for example, a slight break-over near 760 nm for the frosted canopy. The frosted canopies also exhibit a slightly greater peak near 2000 nm; a feature which is used in the modified Cellulose Absorption Index (modCAI) as seen in Table 1.

The 12 spectral indices defined in Table 1 were computed for each measurement (spectrum), and each measurement was associated with an observed presence or absence of frost damage, and a grain yield. To evaluate the response of measured canopy reflectance to frost damage, analysis was performed comparing frost and non-frost damaged datasets acquired on the two dates in 2006 following observed frost (Zadoks growth stages Z65 and Z73), and the transect measured on 13 October 2015 (Z71–75). A subset of the 2015 measurements was selected to avoid wheel

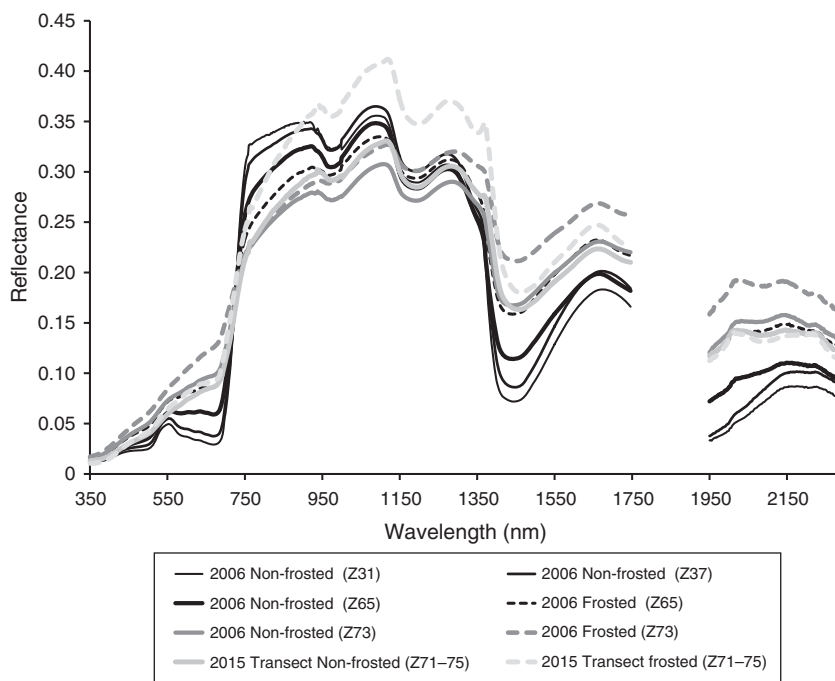


Fig. 2. Reflectance spectra averaged by site and frost exposure.

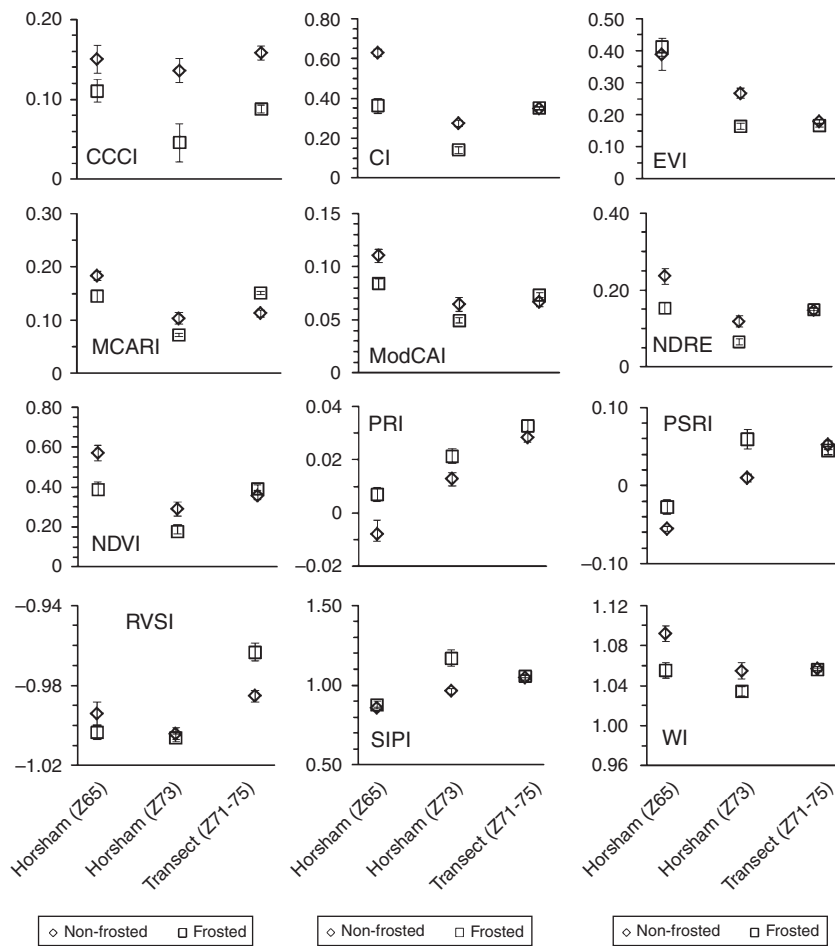


Fig. 3. Average and standard error values for reflectance indices averaged by site and frost exposure.

tracks, excessive mulch areas, and the transition between the frosted and non-frosted canopies. For both the frosted and non-frosted data, the indices show differences between the Z65 and Z73 measurements for 2006, and the Z73 stage measurements for 2006 and 2015 (Fig. 3). Means from 2006 measurements made before frost effects were observed (not shown) demonstrate trends in the indices over growth stages of the crop. To evaluate any differences between frosted and non-frosted canopies, ANOVA was used to make comparisons for each of the three dates (Z65 and Z73 in 2006, and Z71–75 in 2015). The ANOVA results are shown in Table 3. For the 2006 measurements, the non-frosted and frosted values for most indices showed differences ($P < 0.05$) on one or both dates, with the exception of RVSI. For the 2015 transect, MCARI and RVSI showed differences between non-frosted and frosted plots ($P < 0.05$). Over the entire dataset, MCARI was the only index evaluated to show significant differences ($P < 0.05$) across the two crop growth stages and sites.

To analyse all of the 2015 measurements, yield was used as a cumulative indicator of frost damage. For each of the 12 indices, a correlation between the measured index value and

Table 3. ANOVA results for reflectance indices between non-frosted and frosted plots

Index (from Table 1)	F Statistic and P-value		
	24 Oct. 2006 (Z65)	8 Nov. 2006 (Z73)	13 Oct. 2015 (Z71–75)
CI	7.79, 0.018	8.53, 0.017	0.05, 0.825
EVI	0.19, 0.674	35.75, <0.001	2.58, 0.132
MCARI	6.98, 0.023	6.20, 0.034	30.44, <0.001
NDRE	9.09, 0.012	8.96, 0.015	0.08, 0.788
NDVI	10.74, 0.007	7.65, 0.022	3.08, 0.103
PRI	4.64, 0.054	5.67, 0.041	2.04, 0.177
PSRI	11.81, 0.006	15.31, 0.004	0.79, 0.389
RVSI	1.31, 0.277	0.32, 0.587	16.48, 0.001
SIPI	0.75, 0.405	17.68, 0.002	0.21, 0.657
WI	10.01, 0.009	4.38, 0.066	0.19, 0.667
modCAI	9.22, 0.011	3.98, 0.077	2.17, 0.165
CCI	2.51, 0.142	10.82, 0.01	52.01, <0.001
<i>n Frosted</i>	5	5	8
<i>n Non-frosted</i>	8	6	7

the corresponding yield was performed using the 31 rows. The correlation results are shown in Table 4. RVSI and EVI resulted in the highest r values (-0.69 and 0.63 , respectively), whereas the correlations between the remaining indices and yield resulted in r values less than 0.6 . Plots of index values for RVSI and EVI with the corresponding yields along the transect are shown in Fig. 4. The negative correlation between RVSI and yield can be seen in the transect plot, and suggests slight shifts in the inflection point of the red-edge at or near 732 nm. EVI is positively correlated with yield, which would indicate that generally the portion of green biomass decreased along the transect along with the decrease in yield.

For the hyperspectral reflectance data, the utility of a range of associated indices appeared variable across the two experimental sites where frost was observed in-crop. The indices that show significant differences ($P < 0.05$) between measurements of frosted and non-frosted canopies for the 2006 data do not concur with observations taken in 2015. Several of the indices have mean values (for frosted and non-frosted), which appear to reverse between the 2006 and 2015 datasets. In particular, although MCARI shows significant ($P < 0.05$) frost effects for the 2006 and 2015, the treatment means (non-frosted and frosted) are reversed for 2015 compared with 2006.

Table 4. Correlations between yield and reflectance indices for 31 transect plots

Index (from Table 1)	N	r	p
CCCI	31	0.40	0.03
CI	31	0.10	0.60
EVI	31	0.63	<0.001
MCARI	31	-0.32	0.08
modCAI	31	-0.19	0.30
NDRE	31	0.11	0.57
NDVI	31	-0.02	0.93
PRI	31	-0.37	0.04
PSRI	31	-0.25	0.18
RVSI	31	-0.69	<0.001
SIPI	31	-0.46	0.01
WI	31	0.34	0.07

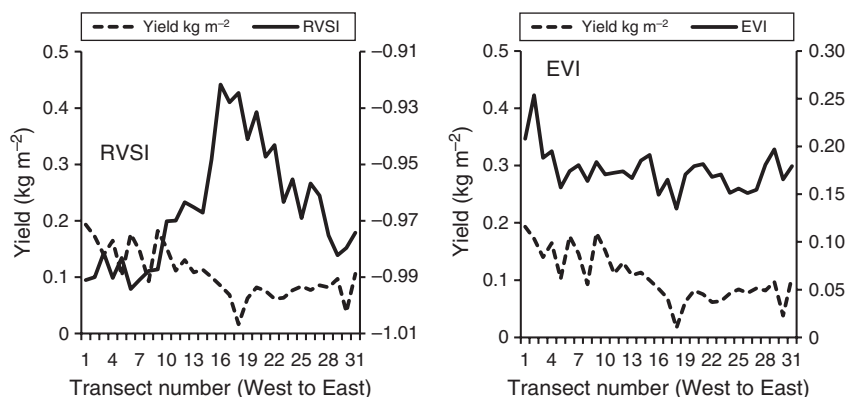


Fig. 4. Plot of index values and yields along the 2015 transect (from non-frosted to heavily frost affected) for RVSI and EVI.

Fluorescence response to frost

Fluorescence measurement using the hand-held active light fluorometer as described in section 2.2 was used for the Kewell site transect on two dates in 2015 following observed frost damage, representing wheat growth stages Z68 and Z71–75. The measurements were used to generate the indices described in Table 2. Multiple measurements were made along a 3-m section of each of the 31 rows of the transect. All of the measurements, and their corresponding indices, were averaged at each of the 31 sites. The indices were then evaluated with respect to the corresponding yield measured at each of the 31 rows.

Five of the indices and the corresponding yield values for the transects are plotted in Fig. 5. These results show that the index FLAV (an indicator for flavinols) and SFR_G (an indicator for chlorophyll) appear to track with yield, and are consistent across the two dates. SFR_R (not shown) is similar to SFR_G. NBI1, an indicator of canopy nitrogen, appears to be negatively correlated with yield along the transect. The other two NBI indices (NBI_G and NBI_R) have similar trends. Two of the indices, BFRR_uv (an indicator for water stress) and ANTH_RB (an index of anthocyanins) do not appear to trend with yield. Results for ANTH_RG (not shown) are similar to ANTH_RB.

Correlation analysis was performed to evaluate the relation between the indices and yield for the 31 rows (Table 5). These results are consistent with the apparent trends shown in Fig. 5. FLAV and the chlorophyll indices SFR_G and SFR_R were positively correlated with yield, as the trends in Fig. 5 would indicate. The index FLAV has the highest correlation coefficient (r value) on each of the two dates, 0.91 and 0.90 respectively. SFR_G had r values of 0.76 and 0.80 for the two dates, whereas the other chlorophyll index had slightly poorer r values of 0.72 and 0.64 . The nitrogen indices NBI_G, NBI_R, and NBI1 were all negatively correlated with yield. NBI_R had the largest value of r , -0.80 for the Z68 measurements, and -0.86 for the Z73 measurements.

Comparison of the reflectance and fluorescence results

Several of the spectral and fluorescence indices can be classed into three categories of related indices: chlorophyll indices, N indices,

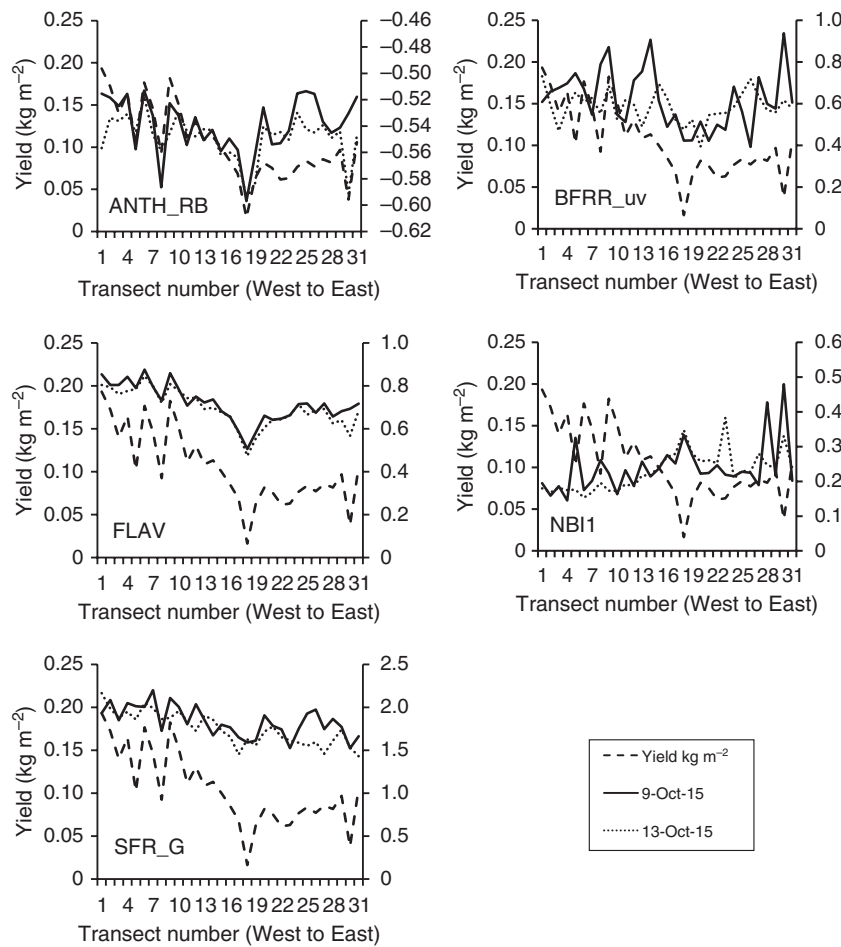


Fig. 5. Corresponding grain yield and fluorometer measurements along a transect (west–east) of 31 rows for two dates (Z61–69, Z71–75) following the first observation of frost.

Table 5. Correlations between yield and fluorometer indices

Index	N	Z68		Z71–75	
		r	p	r	p
ANTH_RB	31	0.56	0.0011	0.61	<0.001
ANTH_RG	31	0.39	0.0288	0.10	0.6048
BFRR_uv	31	0.33	0.0736	0.33	0.0707
FLAV	31	0.91	<0.001	0.90	<0.001
NBI_G	31	−0.63	<0.001	−0.56	<0.0011
NBI_R	31	−0.80	<0.001	−0.86	<0.001
NBI1	31	−0.61	<0.001	−0.83	<0.001
SFR_G	31	0.76	<0.001	0.80	<0.001
SFR_R	31	0.72	<0.001	0.64	<0.001

and water stress. Comparisons across the spectral reflectance and active fluorescence indices may provide insights into characteristics that are indicative of frost damage.

The spectral reflectance index CI, a representative chlorophyll index, indicated a significant effect of frost treatment ($P > 0.05$) for both dates in 2006, but not for 2015. For the 2006 dates, the CI values were higher for the non-frosted plants. The correlation with

yield in 2015 was poor ($r = 0.10$). However, the fluorometer indices SFR_G and SFR_R had relatively high correlations with yield in 2015 on both dates, with correlation coefficient values ranging from 0.64 to 0.80. The CI 2006 results, as well as the positive relationship between the fluorometer chlorophyll indices and yield, suggest that the chlorophyll content of plants decreases with increases in visual symptoms of frost damage.

Canopy N indices produced inconsistent results. The spectral reflectance index RVS1 was slightly higher for non-frosted plants in 2006, but lower in 2015. RVS1 and the three canopy N indices from active fluorescence (NBI_G, NBI_R, and NBI1) all had negative correlations with yield for the 2015 transect, and by association a positive relationship with frost damage. CCC1 values for all dates in 2006 and 2015 were higher for non-frosted plants than frosted plants. However, the correlation with yield along the 2015 transect was poor ($r = 0.40$).

The water stress indices did not appear to respond to differences in frost damage. The spectral reflectance index WI differentiated non-frosted and frosted plants (at $P < 0.05$) only on one date (Z65 in 2006). The correlation between yield and WI in 2015 was quite low ($r = 0.34$). Likewise, BFRR_uv resulted in poor correlations with yield in 2015, with $r = 0.33$ for both dates.

Table 6. Classification of frost using FLAV as discriminant variable

Row labels	Frosted	Non-frosted	Grand total
Frosted	39	3	42
Non-frosted	2	18	20
Grand total	41	21	57/62 (92% overall accuracy)

Application to in-season, agronomic management

A rapid method to generate crop estimates of the presence and spatial extent of frost damage could be used as an agronomic management tool. This would require the ability to classify measurements (proximal measurements or image pixels) into classes of frosted or non-frosted. Given the strong correlation with yield for both dates, the fluorescence index FLAV was selected to evaluate whether it could be used to classify the canopy as frost affected or not. The classification was performed using discriminant analysis for the 2015 transect data. The 62 measurements, comprised of 31 rows over two dates, were used for the test. The training set consisted of eight frosted and eight non-frosted samples randomly selected from the two dates, for a total of 16 measurements. The program was run with the option to re-classify the initial 16 measurements, along with the remaining 46 measurements, according to the training set results. The classification results are shown in Table 6. The rows represent the observed frost status (frosted or non-frosted), whereas the columns represent the classified values. Out of 62 total measurements, two measurements were incorrectly classified as frosted, and three were incorrectly classified as non-frosted. The overall classification accuracy, defined as the number of correctly classified measurements (57) divided by the total number (62) was 92%.

The present study was not able to provide insight into how rapidly the sensors could detect frost damage before detection with the naked eye, as the survey data constituted a transect based on early visual symptoms. This data did however provide us an important insight into what sensors and/or indices may be sensitive to detecting early frost damage in-crop.

Next steps towards application to agronomic management

This research is the first step in evaluating non-destructive proximal and remote sensing methods to detect frost damage in wheat around anthesis for the purpose of developing tools for rapid, spatial assessment of frost-affected crops. These initial results indicated that the fluorescence index FLAV was the most responsive to frost damage of the fluorescence and reflectance indices evaluated. Additional datasets are required to validate the use of active fluorimeters against observed damage, and to evaluate pre-visual symptoms. The research to follow will be critical to determining key requirements for the technology needed. The scale of measurements required (e.g. proximal versus remote sensing), as well as the specific sensor(s) and indices will inform the platform, sensors, and measurement approach. For example, passive reflectance or canopy chlorophyll could be measured from imaging systems flown on a UAV. Proximal sensors may require manual operation, or installation on a ground-based vehicle.

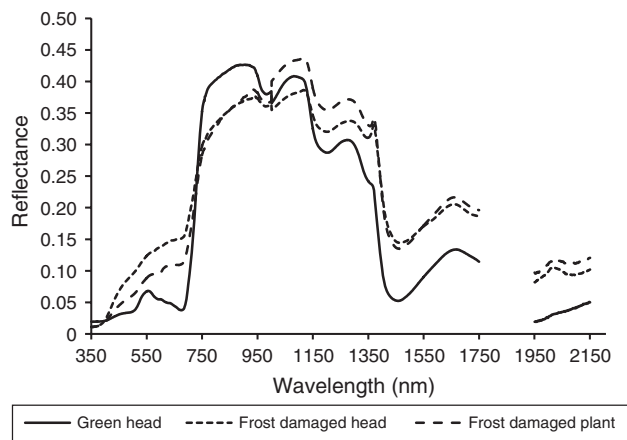


Fig. 6. Spectral reflectance acquired slightly after Z65 for a non-frosted wheat head (solid line), frost-damaged wheat head (short dash), and frost-damaged wheat plant (long dash).

Other key research questions include what nominal scale of measurements are required, and for which portions of the plant canopy. In this study, the fluorometer was used to measure the wheat heads, whereas reflectance measurements were made to measure the top of the canopy, which included the flag leaves and wheat heads. Fig. 6 shows example spectra acquired on 26 October 2006 as part of the same experiment described in section 2.1, 2 days after the Z65 dataset. The reflectance spectrum measured from the frost-damaged wheat head was more distinctive than the canopy level spectrum. A spectral library, which includes scales from the wheat heads to the canopy level, would address the issue of scale for reflectance indices.

Another research question is how robust (over space and time) any relationships are between frost damage and index response. Some of the spectral reflectance indices (e.g. MCARI, RVSI) reversed the relationship between means for frosted and non-frosted plants between the 2006 and 2015 data. If a classification approach is used, how localised will the calibration and validation need to be to differentiate frost-damaged plants?

The ultimate objective is to detect frost damage before the onset of visual damage. In order to acquire this data, experiments must be designed to induce frost damage and/or protect control plants from frost.

Conclusions

Fluorescence using an active light source was clearly superior to passive spectral sensing for detection of frost damage in this set of data. Reflectance is influenced by a multitude of higher order factors including plant architecture and variable lighting conditions. It may be that as fluorescence measures characteristics of photosynthesis more directly, this is more universally applicable and free of artefacts associated with plant structure and environmental lighting. Clearly more work is required, including testing reflectance indices using active light sources. However, this research shows the value of active sensing for frost detection.

Operationally, use of an active sensor may be more challenging as it is highly desirable to be able to fly over a crop (with a UAV

or satellite) and map frost damage. Using a UAV does not preclude the use of an active sensor but the requirements are more demanding in terms of power and weight. Given the rapid development of these systems, however, this may not be a hindrance within a few years.

Acknowledgements

We would like to acknowledge the programs 'Improving practices and adoption through strengthening D and E capability and delivery in the Southern region (RRA)' program, 'Our Rural Landscape', and the 'National Frost Initiative' for supporting this work. Funds were provided by the Grains Research and Development Corporation and the State of Victoria Department of Economic Development, Jobs, Transport and Resources. We also thank growers I. Ruwoldt and R. Cole for providing commercial wheat crop for experimental purposes.

References

- Agati G, Foschi L, Grossi N, Guglielminetti L, Cerovic ZG, Volterriani M (2013) Fluorescence-based versus reflectance proximal sensing of nitrogen content in *Paspalum vaginatum* and *Zoysia matrella* turfgrasses. *European Journal of Agronomy* **45**, 39–51.
- Al-Issawi M, Rihan HZ, El-Sarkassy N, Fuller MP (2013) Frost hardiness expression and characterisation in wheat at ear emergence. *Journal of Agronomy & Crop Science* **199**, 66–74. doi:10.1111/j.1439-037X.2012.00524.x
- Bürling K, Hunsche M, Noga G (2011) Use of blue-green and chlorophyll fluorescence measurements for differentiation between nitrogen deficiency and pathogen infection in winter wheat. *Journal of Plant Physiology* **168**, 1641–1648. doi:10.1016/j.jplph.2011.03.016
- Bürling K, Cerovic ZG, Cornic G, Ducruet J-M, Noga G, Hunsche M (2013) Fluorescence-based sensing of drought-induced stress in the vegetative phase of four contrasting wheat genotypes. *Environmental and Experimental Botany* **89**, 51–59. doi:10.1016/j.envexpbot.2013.01.003
- Clarke TR, Moran MS, Barnes EM, Pinter PJ, Qi J (2001) Planar domain indices: A method for measuring a quality of a single component in two-component pixels. In 'IGARSS 2001. Scanning the Present and Resolving the Future. Proceedings IEEE International Geoscience and Remote Sensing Symposium'. Sydney, NSW, 9–13 July 2001. Vol. 3, pp. 1279–1281. <http://ieeexplore.ieee.org/stamp/stamp.jsp?tp=&number=976818&isnumber=21047>
- Cromeey M, Wright D, Boddington H (1998) Effects of frost during grain filling on wheat yield and grain structure. *New Zealand Journal of Crop and Horticultural Science* **26**, 279–290. doi:10.1080/01140671.1998.9514065
- Daughtry CST (2001) Discriminating crop residues from soil by shortwave infrared reflectance. *Agronomy Journal* **93**, 125–131. doi:10.2134/agronj2001.931125x
- Daughtry CST, Walthall CL, Kim MS, de Colstoun EB, McMurtrey JE III (2000) Estimating corn leaf chlorophyll concentration from leaf and canopy reflectance. *Remote Sensing of Environment* **74**, 229–239. doi:10.1016/S0034-4257(00)00113-9
- de Leeuw J, Vrieling A, Shee A, Atzberger C, Hadgu K, Biradar C, Keah H, Turvey C (2014) The potential and uptake of remote sensing in insurance: A review. *Remote Sensing* **6**, 10888–10912. doi:10.3390/rs61110888
- Fernandez-Jaramillo AA, Duarte-Galvan C, Contreras-Medina LM, Torres-Pacheco I, Romero-Troncoso RdJ, Guevara-Gonzalez RG, Millan-Almaraz JR (2012) Instrumentation in developing chlorophyll fluorescence biosensing: A review. *Sensors* **12**, 11853–11869. doi:10.3390/s120911853
- Fitzgerald G, Rodriguez D, O'Leary G (2010) Measuring and predicting canopy nitrogen nutrition in wheat using a spectral index – the canopy chlorophyll content index (CCCI). *Field Crops Research* **116**, 318–324. doi:10.1016/j.fcr.2010.01.010
- Flower K, Boruss B, Nansen C, Jones H, Thompson S, Lacoste C, Murphy M (2014) Proof of concept: remote sensing frosted-induced stress in wheat paddocks. Grains Research and Development Corporation, Canberra.
- Gamon JA, Peñuelas J, Field CB (1992) A narrow-waveband spectral index that tracks diurnal changes in photosynthetic efficiency. *Remote Sensing of Environment* **41**, 35–44. doi:10.1016/0034-4257(92)90059-S
- Ghozlen NB, Cerovic ZG, Germain C, Toutain S, Latouche G (2010) Non-destructive optical monitoring of grape maturation by proximal sensing. *Sensors* **10**, 10040–10068. doi:10.3390/s101110040
- Gitelson AA, Keydan GP, Merzlyak MN (2006) Three-band model for noninvasive estimation of chlorophyll, carotenoids, and anthocyanin contents in higher plant leaves. *Geophysical Research Letters* **33**, L11402.
- Huete A, Didan K, Miura T, Rodriguez EP, Gao X, Ferreira LG (2002) Overview of the radiometric and biophysical performance of the MODIS vegetation indices. *Remote Sensing of Environment* **83**, 195–213. doi:10.1016/S0034-4257(02)00096-2
- Jones HG (2014) 'Plants and microclimate: a quantitative approach to environmental plant physiology.' (Cambridge University Press: Cambridge, UK)
- Juttner J (2014) Focus on Frost. GRDC Ground Cover. Grains Research and Development Corporation, Canberra.
- Kokaly RF, Clark RN (1999) Spectroscopic determination of leaf biochemistry using band-depth analysis of absorption features and stepwise multiple linear regression. *Remote Sensing of Environment* **67**, 267–287. doi:10.1016/S0034-4257(98)00084-4
- Macedo-Cruz A, Pajares G, Santos M, Villegas-Romero I (2011) Digital image sensor-based assessment of the status of oat (*Avena sativa* L.) crops after frost damage. *Sensors* **11**, 6015–6036. doi:10.3390/s110606015
- Marcellos H, Single W (1984) Frost injury in wheat ears after ear emergence. *Functional Plant Biology* **11**, 7–15. doi:10.1071/PP9840007
- Merton RN (1998) Monitoring community hysteresis using spectral shift analysis and the red-edge vegetation stress index. In 'Seventh Annual JPL Airborne Earth Science Workshop'. NASA Jet Propulsion Laboratory, Pasadena, California, USA, 12–16 January 1998.
- Merzlyak MN, Gitelson AA, Chivkunova OB, Rakitin VYU (1999) Non-destructive optical detection of pigment changes during leaf senescence and fruit ripening. *Physiologia Plantarum* **106**, 135–141. doi:10.1034/j.1399-3054.1999.106119.x
- Peel MC, Finlayson BL, McMahon TA (2007) Updated world map of the Köppen-Geiger climate classification. *Hydrology and Earth System Sciences* **11**, 1633–1644. doi:10.5194/hess-11-1633-2007
- Peñuelas J, Baret F, Filella I (1995) Semi-empirical indices to assess carotenoids/chlorophyll a ratio from leaf spectral reflectance. *Photosynthetica* **31**, 221–230.
- Peñuelas J, Pinol J, Ogaya R, Filella I (1997) Estimation of plant water concentration by the reflectance water index WI (R900/R970). *International Journal of Remote Sensing* **18**, 2869–2875. doi:10.1080/014311697217396
- Peters AJ, Griffin SC, Vina A, Ji L (2000) Use of remotely sensed data for assessing crop hail damage. *Photogrammetric Engineering and Remote Sensing* **66**, 1349–1355.
- Rapacz W, Woźniczka A (2009) A selection tool for freezing tolerance in common wheat using the fast chlorophyll a fluorescence transient. *Plant Breeding* **128**, 227–234. doi:10.1111/j.1439-0523.2008.01566.x
- Rapacz M, Sasal M, Gut M (2011) Chlorophyll fluorescence-based studies of frost damage and the tolerance for cold-induced photoinhibition in freezing tolerance analysis of triticale (*×Triticosecale* Wittmack). *Journal of Agronomy & Crop Science* **197**, 378–389. doi:10.1111/j.1439-037X.2011.00472.x
- Rizza F, Pagani D, Stanca AM, Cattivelli L (2001) Use of chlorophyll fluorescence to evaluate the cold acclimation and freezing tolerance of

- winter and spring oats. *Plant Breeding* **120**, 389–396. doi:10.1046/j.1439-0523.2001.00635.x
- Rouse JW, Jr, Haas RH, Schell JA, Deering DW (1974) Monitoring vegetation systems in the Great Plains with ETRS. In 'Third Earth Resources Technology Satellite-1 Symposium'. 10–14 Dec. 1973. Vol. 1, Technical Presentations, NASA SP-351. (Eds SC Freden, EP Mercanti, MA Becker) (NASA: Washington, DC)
- Silleos N, Perakis K, Petsanis G (2002) Assessment of crop damage using space remote sensing and GIS. *International Journal of Remote Sensing* **23**, 417–427. doi:10.1080/01431160110040026
- VSN International (2011) 'GENSTAT for Windows.' 14th edn. (VSN International: Hemel Hempstead, UK)
- Wahlquist A (2012) Researchers probe warming climate frost puzzle. GroundCover, Grains Research and Development Corporation, ACT, Australia.
- Wang B, Liu DL, Asseng S, Macadam I, Yu Q (2015) Impact of climate change on wheat flowering time in eastern Australia. *Agricultural and Forest Meteorology* **209–210**, 11–21. doi:10.1016/j.agrformet.2015.04.028
- White C, and GRDC and Agriculture Western Australia (2000) 'Cereals – frost identification: the back pocket guide.' (Agriculture Western Australia: Perth)
- Wu Q, Zhu D, Wang C, Ma Z, Wang J (2012) Diagnosis of freezing stress in wheat seedlings using hyperspectral imaging. *Biosystems Engineering* **112**, 253–260. doi:10.1016/j.biosystemseng.2012.04.008
- Zadoks JC, Chang TT, Konzak CF (1974) A decimal code for the growth stages of cereals. *Weed Research* **14**, 415–421. doi:10.1111/j.1365-3180.1974.tb01084.x
- Zheng B, Chenu K, Fernanda Dreccer M, Chapman SC (2012) Breeding for the future: what are the potential impacts of future frost and heat events on sowing and flowering time requirements for Australian bread wheat (*Triticum aestivum*) varieties? *Global Change Biology* **18**, 2899–2914. doi:10.1111/j.1365-2486.2012.02724.x
- Zheng B, Chapman SC, Christopher JT, Frederiks TM, Chenu K (2015) Frost trends and their estimated impact on yield in the Australian wheatbelt. *Journal of Experimental Botany* **66**, 3611–3623. doi:10.1093/jxb/erv163